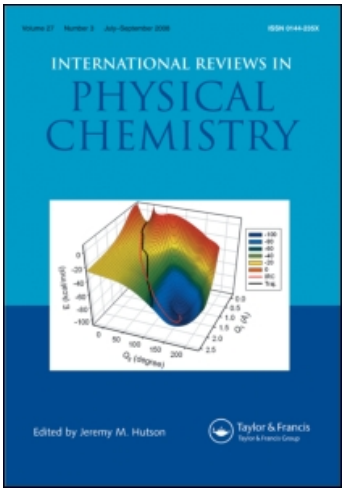

International Reviews in Physical Chemistry
Publication details, including instructions for authors and subscription information:
http://www.informaworld.com/smpp/title~content=t713724383

Millimetre wave spectroscopy of high Rydberg states

F. Merkt; A. Osterwalder

Online publication date: 26 November 2010

To cite this Article Merkt, F. and Osterwalder, A.(2002) 'Millimetre wave spectroscopy of high Rydberg states', International Reviews in Physical Chemistry, 21: 3, 385 — 403
To link to this Article: DOI: 10.1080/01442350210151641
URL: http://dx.doi.org/10.1080/01442350210151641

INT. REVIEWS IN PHYSICAL CHEMISTRY, 2002
VOL. 21, NO. 3, 385–403

Taylor & Francis
Taylor & Francis Group

Millimetre wave spectroscopy of high Rydberg states

F. MERKT and A. OSTERWALDER
Physical Chemistry, ETH Zurich, CH-8093 Zurich, Switzerland

We have recently developed high-resolution vacuum ultraviolet laser sources and combined these with millimetre waves in double-resonance experiments to achieve a spectral resolution of up to 60 kHz in the spectra of high Rydberg states. The article describes the main features of our experimental procedure and presents studies in which we have used millimetre wave spectroscopy (a) to obtain information on the energy level structure, including the spin–orbit and hyperfine structure, of atomic Rydberg states at high principal quantum numbers n, (b) to record spectrally resolved spectra of the high Rydberg states ($n \geq 100$) detected in pulsed-field-ionization zero-kinetic-energy photoelectron spectra, (c) to measure stray electric fields and ion concentrations in the gas phase, (d) to test and improve the selectivity of the electric field ionization of high Rydberg states and (e) to observe for the first time the hyperfine structure in high-n, low-l molecular Rydberg states.

Contents

1. Introduction

High-resolution spectroscopy of atomic Rydberg states has been a very fruitful field of research for many years and has provided a detailed understanding of their physical properties [1–3]. For experimental convenience the vast majority of high-resolution spectroscopic investigations of atomic Rydberg states have been limited to systems that can be studied using visible or ultraviolet (UV) laser technology, i.e. metal atoms that possess low-lying ionization potentials (see [1, 2] and references

International Reviews in Physical Chemistry ISSN 0144–235X print/ISSN 1366–591X online © 2002 Taylor & Francis Ltd
http://www.tandf.co.uk/journals
DOI: 10.1080/01442350210151641

therein), or rare gas atoms that can conveniently be prepared in metastable states (see, for instance, [4, 5]).

Spectroscopic studies on atomic Rydberg states are typically performed in two distinct frequency ranges: visible or UV radiation is used to measure Rydberg spectra starting from the ground electronic state or from a long-lived metastable state. Microwaves or millimetre waves are used to measure, at very high resolution, small energy differences between neighbouring Rydberg states [6], between fine or even hyperfine structure components of a given (n, l) Rydberg state [7, 8] or between neighbouring Stark states [9]. Of particular importance for the work presented here was the work of Fabre *et al*. [10] who used millimetre waves to record spectra of the Na atom between $n = 20$ and $n = 40$ at a spectral resolution of $\approx$1 MHz.

Spectroscopic studies of Rydberg states of high principal quantum number $n \gg 50$ require a high spectral resolution and considerable care in controlling experimental conditions. Noteworthy examples of high-resolution spectroscopy of very high atomic Rydberg states are the studies of Dunning and coworkers on Rydberg states of the potassium atom [12], of Hotop and coworkers on Rydberg states of the argon atom [4, 13–15], of Beigang *et al*. on Rydberg states of the strontium atom [16, 17] and of Neukammer *et al*. on high Rydberg states of the barium atom [18].

Almost no high-resolution spectroscopic information is currently available on high Rydberg states of other atoms, and, with the exception of microwave measurements on high angular momentum Rydberg states of H_2 at $n = 10$ and 27 [19–22], nothing is known experimentally of the details of the energy level structure of high molecular Rydberg states. Several reasons may be put forward to explain this lack of information. The optically accessible low-l Rydberg states of molecules decay rapidly by predissociation and/or autoionization and are generally believed to be too short lived to be interesting candidates for high-resolution spectroscopic investigations. Moreover, the Rydberg spectrum of most small molecules lies in the vacuum ultraviolet (VUV) and is not easily accessible by single-photon laser spectroscopy.

We report on a generalization of earlier spectroscopic measurements on Rydberg states of atoms with low ionization potentials to other atoms and molecular systems. Our experimental procedure relies on the use of narrow-bandwidth tunable lasers in the VUV (tunable range 10–19.7 eV [23], bandwidth 1 μeV or 250 MHz [24]) to prepare an initial population of long-lived high Rydberg states directly from the ground state and of millimetre waves to record spectra of transitions from the initially prepared Rydberg states to neighbouring Rydberg states at a resolution of better than 1 MHz [25].

Our initial motivation to study high Rydberg states spectroscopically at high resolution had its origin in the early 1990s when pulsed-field-ionization zero-kinetic-energy (PFI–ZEKE) photoelectron spectroscopy revealed the existence of surprisingly long-lived (lifetimes of more than 10 μs) high Rydberg states (with $n \geq 100$) in a wide range of atomic and molecular systems [26–30]. Possible causes for these long lifetimes have been discussed, and are still discussed, in the literature and include intramolecular energy redistribution processes [27, 31] and Stark mixing by weak homogeneous and inhomogeneous stray fields (see for instance [28, 32–36]). So far, no detailed spectroscopic information is available that could be used to determine conclusively the origin of the long lifetimes observed experimentally. Millimetre wave spectroscopy is a convenient way to obtain this information. It also represents

an attractive method to exploit the long lifetimes for high-resolution spectroscopy of electronically highly excited states.

Next to fundamental investigations of the properties of high Rydberg states, the use of millimetre wave spectroscopy in our laboratory has recently enabled us to carry out quantitative measurements of stray electric fields [37] and ion concentrations [38], to exploit the field ionization dynamics of high Rydberg states to improve the resolution of PFI–ZEKE photoelectron spectroscopy to better than 0.06 cm^{-1} [39] and to make progress towards resolving the hyperfine structure in molecular ions by high Rydberg state spectroscopy and PFI techniques [40, 41]. The present article reviews our recent progress with emphasis on the experimental procedure.

2. Experimental procedure

The study of high Rydberg states poses several experimental challenges: First, the spectral density of Rydberg states scales with n^3 and renders a high experimental resolution at high n values imperative. Then, the Rydberg spectrum of most small-sized molecules lies in the vacuum ultraviolet ($\lambda \leq 200$ nm) or even in the extreme ultraviolet (XUV, $\lambda \leq 105$ nm) where Doppler broadening becomes a limitation to the energy resolution. Finally, the extreme sensitivity of high Rydberg states to even small external perturbations (the polarizability of Rydberg states scales as n^7) can easily falsify high-resolution spectroscopic measurements and necessitates the implementation of reliable diagnostic tools for the determination and elimination of weak stray electric fields.

VUV laser spectroscopy is well suited to study Rydberg states up to approximately $n = 100$. Over recent years we have constructed two broadly tunable VUV lasers for our studies of high Rydberg states. The first one, which has been used for most studies summarized here, is tunable from 10 to 19.6 eV with a bandwidth of 0.1 cm^{-1} [23, 42]. Very recently, we have developed a second laser system, tunable from 9 to 17 eV with a bandwidth better than 250 MHz (0.008 cm^{-1}) [24]. However, intrinsic limitations imposed by the bandwidth of these laser sources and by Doppler broadening prevent the investigation of the highest Rydberg states and the obtaining of the finer details of the energy level structure.

To obtain such details, we use millimetre waves tunable in the range 120–180 GHz (4–6 cm^{-1}) in combination with VUV radiation in double-resonance experiments [25]. In these experiments, the frequency of the VUV laser is held fixed on a given resonance to prepare a population in a selected Rydberg state. The millimetre waves, which are produced by a broadly tunable frequency-stabilized backward wave oscillator, are scanned and induce transitions from the selected Rydberg state to neighbouring Rydberg states. Because the bandwidth of the millimetre wave radiation is less than 1 kHz (3×10^{-8} cm^{-1}) and the Doppler broadening in the wavenumber range 4–6 cm^{-1} is approximately 20 000 times less than at 100 000 cm^{-1}, more than three orders of magnitude can be gained in the resolution. The millimetre wave transitions are detected by selective field ionization (SFI) which enables a high sensitivity and a background free detection. An additional advantage of millimetre waves compared with microwaves is that they can be directed 'optically' through the measurement region by using suitable lenses or reflecting mirrors and do not require the use of waveguides and resonant cavities.

The maximum resolution that can be reached is limited by the transit times of the molecules through the millimetre wave excitation region, and linewidths of 60 kHz

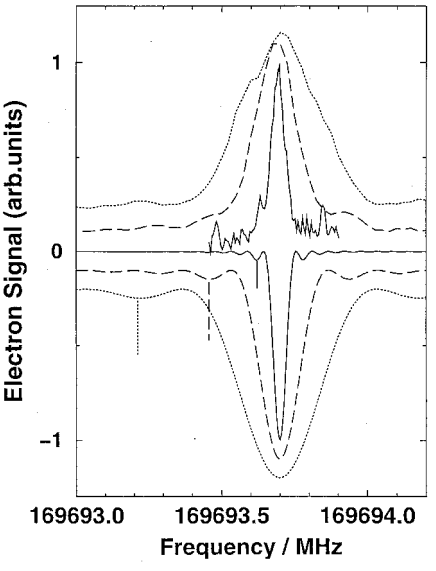

Figure 1. The effect of the delay between laser excitation and delayed PFI on the line shape of millimetre wave transitions. The full, broken and dotted lines show spectra of the $93p[3/2](J=1) \quad 77d[3/2](J'=1)$ transition obtained with delay times Δt of 18 μs, 6 μs and 3 μs respectively. The inverted traces represent calculated line profiles.

have been measured in an skimmed supersonic expansion of atomic krypton [37]. The linewidths can be varied to match the experimental needs by adjusting the measurement time, i.e. the time between the laser pulse and the application of the pulsed electric field as is illustrated in figure 1. The figure shows three recordings of the $93p[3/2](J=1) \quad 77d[3/2](J'=1)$ transition in krypton obtained with measurement times Δt of 3 μs (dotted line, full width at half-maximum (FWHM) of 350 kHz), 6 μs (broken line, FWHM of 150 kHz) and 18 μs (full line, FWHM of 60 kHz). (Argon and krypton Rydberg states are labelled in *jl* coupling, e.g. $(\tilde{n}p)^5 nl'[k](J)$: $(\tilde{n}p)^5$ represents the electronic configuration of the core, n and l denote the principal and the orbital angular momentum quantum number of the Rydberg electron, the optional $'$ denotes the series converging to the upper $^2P_{1/2}$ spin–orbit threshold (instead of the lower $^2P_{3/2}$ spin–orbit threshold), J is the total angular momentum quantum number and k represents the angular momentum quantum number associated with the vector $\boldsymbol{k} = \boldsymbol{J} - \boldsymbol{s}$, where $\boldsymbol{s}$ is the Rydberg electron spin angular momentum vector. See [43].) The inverted traces represent calculated line profiles using the intensity distribution function [44]

$$I(\nu) = I_0 \,\mathrm{sinc}^2(\pi\nu\,\Delta t). \tag{1}$$

The spectral profiles are characterized by side bands, the first one of which is located at a distance $\Delta\nu = 1/\Delta t$ from the main peak. These side bands are observed at the expected positions in the experimental spectra except for the spectrum recorded using a delay time of 18 μs because, at such long delay times, the atoms start exiting the measurement region before the application of the field ionization pulse. Short measurement times, and the associated line broadening, are particularly convenient when searching for spectral lines [40].

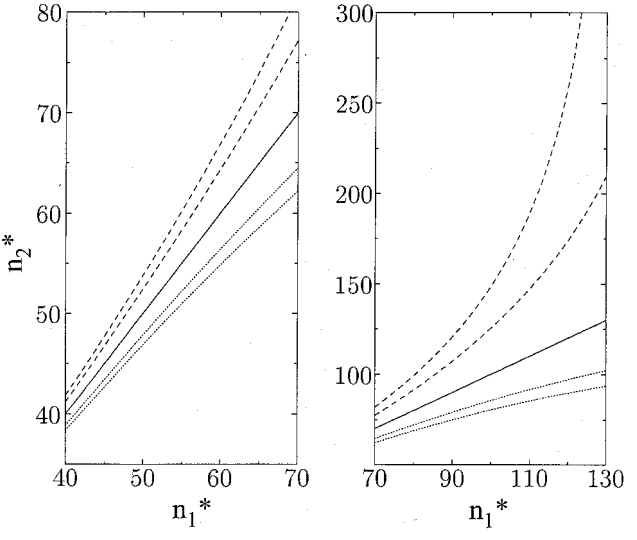

Figure 2. Range of final Rydberg state effective principal quantum number n_2^* that can be reached from an initial Rydberg state of effective principal quantum number n_1^* using a millimetre wave source tunable between 120 and 180 GHz.

Figure 2 gives an overview of the range of effective quantum numbers n^* that can be studied with our millimetre wave source. The effective quantum numbers n_1^* and n_2^* of the initial and final Rydberg states of the millimetre wave transitions are indicated along the horizontal and vertical axes respectively. The diagonal line represents the initial Rydberg states and the two bands of final states correspond to transitions to higher or lower Rydberg states. Transitions to long-lived Rydberg states located within these two bands are conveniently detected by SFI.

The most effective way of recording millimetre wave spectra from a selected Rydberg state with principal quantum number n' is illustrated in figure 3(*b*) and consists of applying a slowly growing electric field pulse and setting detection gates on the time-of-flight (TOF) spectrum of the electrons at the positions expected for the field ionization of the initial and final Rydberg states. The earliest electron signal stems from the field ionization of the Rydberg states of principal quantum number $n_A > n'$ that have been excited by absorption of millimetre wave radiation. The latest signal in the TOF spectrum corresponds to Rydberg states of principal quantum number $n_{SE} < n'$ produced by stimulated emission. The middle signal in the TOF spectrum enables the monitoring of the population in the initially prepared Rydberg state. As an illustration of this detection method, figure 4 shows millimetre wave spectra recorded simultaneously from the initially prepared $62d[1/2](J' = 1)$ state of argon using a slowly growing pulse with a slew rate of 87.7 V cm^{-1} μs^{-1}. The traces labelled 1, 2, and 3 in the figure correspond to spectra obtained by monitoring the early, late and middle electron signals in the TOF spectrum as a function of the millimetre wave frequency. Not only can transitions to the $67f$ Rydberg states (absorption) and the $57f$ Rydberg states (stimulated emission) be recorded simultaneously in separate traces, but a weak reduction (*c.* 20%) in the field ionization signal of the initial state can also be observed at the positions of these transitions (see figures 4(*b*) and (*c*)). In this way, a complete picture of the interaction

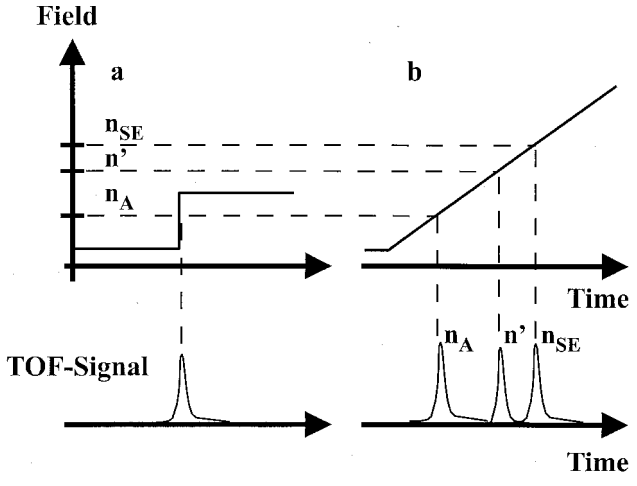

Figure 3. Principle of the detection of millimetre wave transitions by SFI of initial and final states using (*a*) a fast electric field pulse of well-defined amplitude or (*b*) a slowly growing electric field pulse.

of the millimetre waves with the high Rydberg states can be reconstructed. The only disadvantage of this detection method lies in the long duration of the field pulse (*c*. 400 ns in the case illustrated in figure 4) during which millimetre wave transitions are induced in a time-dependent electric field that can lead to an enhanced background signal or field-induced structures in the millimetre wave spectra.

This disadvantage can be avoided by using a rapidly growing electric field pulse with an amplitude chosen such that only the upper Rydberg states (n_A) can be detected (see figure 3(*a*)). However, in molecules, this detection method fails whenever the final state is short lived and decays before the application of the pulsed electric field. In this case, it is more advantageous to monitor the transitions as dips in the SFI signal of the initial state (see figure 11 below).

The millimetre wave transitions, particularly those between Rydberg states of neighbouring principal quantum numbers (Δn small), are very easily saturated and necessitate considerable attenuation of the millimetre wave intensity (typically 50–60 dB, corresponding to intensities of 0.5–5 nW cm^{-2}, for the strongest transitions with initial state principal quantum number around $n = 50$). In general, transitions involving larger Δn changes require higher intensities, but, even for transitions between $n = 115$ and $n = 200$ Rydberg states, attenuation to $\approx$10 μW cm^{-2} or less is necessary to avoid saturation.

Figure 5 illustrates how the millimetre wave intensity influences spectral structures with the example of the $69f[3/2](J = 1, 2) \quad 62d[1/2](J' = 1)$ transitions in argon. The millimetre wave spectra recorded at intensities of *c*. 5 nW cm^{-2} (50 dB), 500 nW cm^{-2} (30 dB), 50 μW cm^{-2} (10 dB) and 0.5 mW cm^{-2} (0 dB) are displayed from top to bottom in figure 5(*b*). In each case the full and broken lines correspond to the field ionization signals of the final and initial states of the transition respectively. Both traces were recorded simultaneously using a slowly growing field ionization pulse (see figure 3). The side panels in figure 5 show the electron TOF spectra obtained at the positions of the lower ($J = 1$, figure 5(*a*)) and upper ($J = 2$, figure 5(*c*)) resonances. In each TOF spectrum the earlier peak stems from the field

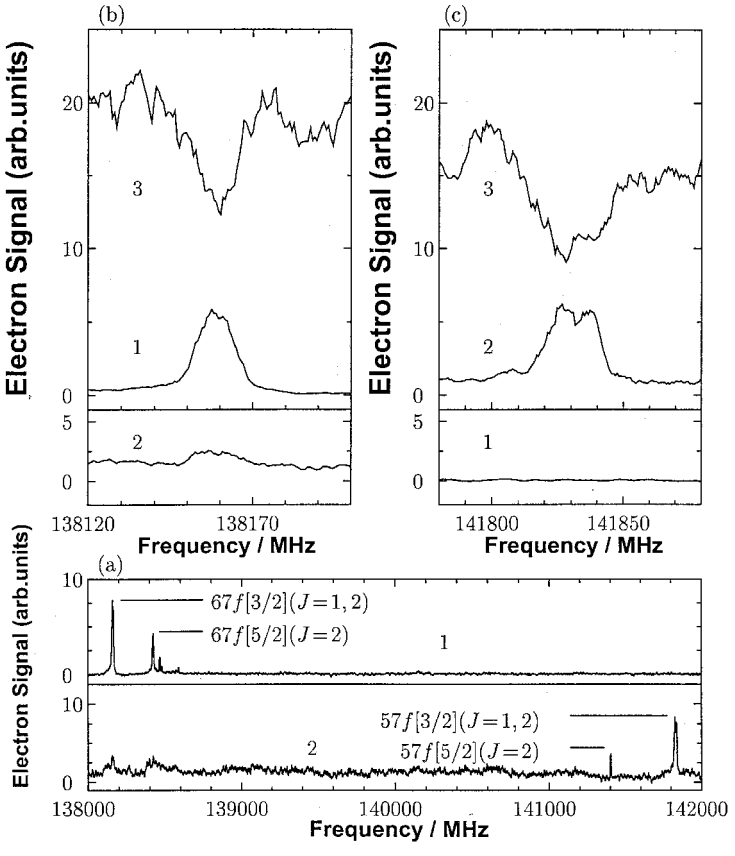

Figure 4. Millimetre wave spectra recorded from the initially prepared $62d[1/2](J'=1)$ state of argon using a slowly growing pulse with a slew rate of $87.7\,\mathrm{V\,cm^{-1}\,\mu s^{-1}}$ and showing transitions to the $67f$ and $57f$ Rydberg states. The traces labelled 1 and 2 correspond to spectra obtained by monitoring the final Rydberg states produced by absorption and stimulated emission respectively of millimetre wave radiation. The trace labelled 3 shows the field ionization signal of the initial Rydberg state. (*b*) and (*c*) show details of the survey spectra of panel (*a*) on an expanded scale.

ionization of the final $n = 69f$ states and the later broader peak from the field ionization of the $n = 62d$ initial state. The broken lines in the side panels represent the integrated electron TOF signals from which the onset of saturation can be determined. As soon as the integrated signals from the initial and final states of the transitions become comparable (i.e. at intensities of approximately $500\,\mathrm{nW\,cm^{-2}}$) a broadening of the transitions becomes noticeable which eventually prevents the observation of resolved spectral structures. The saturation can also be recognized in figure 5(*b*) from the equilibration of the amplitude of the dip in the spectrum of the initial state with that of the peak in the spectrum of the final state. At the highest intensities shown in figure 5 the amplitude of the dips in the spectrum of the initial state becomes larger than 50% of the total PFI signal because the millimetre waves start ionizing the Rydberg states during the measurement time.

The tuning range of 120–180 GHz of the millimetre waves restricts most spectroscopic experiments to n values beyond 40 (see figure 2). At these values of n, transitions between neighbouring Rydberg states that can be efficiently induced by

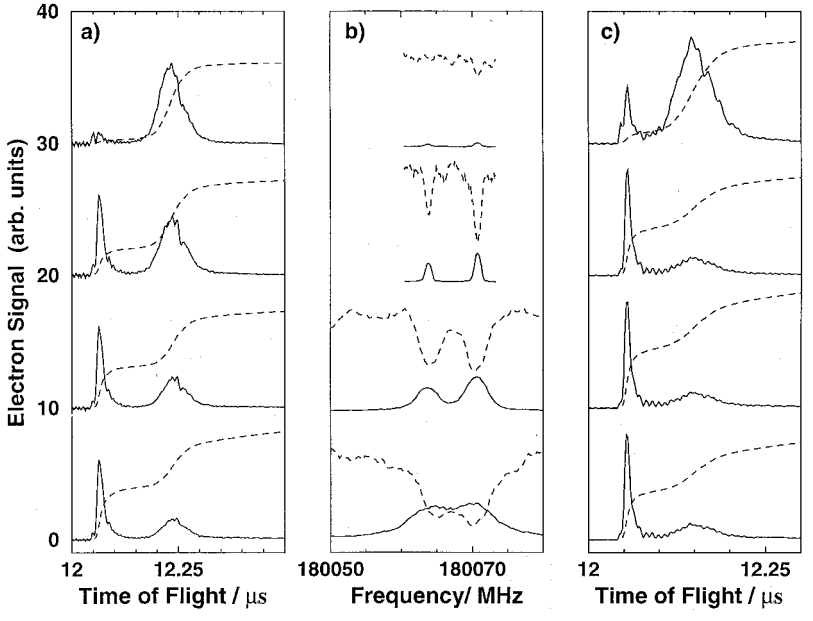

Figure 5. Effect of the millimetre wave intensity on the spectrum of the $69f[3/2](J = 1, 2)$ $62d[1/2](J' = 1)$ transitions in argon. The millimetre wave spectra recorded at intensities of *c.* 5 nW cm^{-2} (50 dB), 500 nW cm^{-2} (30 dB), 50 μW cm^{-2} (10 dB) and 0.5 mW cm^{-2} (0 dB) are displayed from top to bottom in (*b*). In each case the full and broken lines correspond to the field ionization signals of the final and initial states of the transition respectively. The full lines in the side panels show the electron TOF spectra obtained at the position of the lower ($J = 1$, (*a*)) and upper ($J = 2$, (*c*)) resonance and the broken lines show the integrated TOF signals.

millimetre wave radiation have frequencies below 180 GHz. The blackbody radiation density below 180 GHz at 300 K amounts to less than 1/1000 of the maximum intensity at 600 cm^{-1}, and we have so far not observed any significant interference of the blackbody radiation with our measurements.

The position of high Rydberg states can be affected by the pressure shift induced by the presence of foreign gas atoms or molecules within the Rydberg electron orbit [45, 46]. The main contributions to the pressure shift stem from the polarization of the foreign gas particles by the charged ion core, which leads to a shift towards lower energies, and from the scattering of the slow Rydberg electron by the foreign gas particle, which can lead to an energy displacement toward higher or lower energies depending on the phase shift of the scattering wave function. The pressure shift can have pronounced effects on Rydberg spectra recorded from the ground state [2, 45–47] because the initial state of the transition is not affected by the pressure shift. Its effect on millimetre wave transitions between high Rydberg states is much less important because the initial and final Rydberg states are subject to a very similar pressure shift. Indeed the pressure shift becomes independent of n and l at high n because the number of foreign gas particles within the Rydberg electron orbit increases as rapidly as the electron density decreases. Our attempts to observe pressure shifts by millimetre wave spectroscopy have so far remained unsuccessful. The results of one such attempt are illustrated in figure 6 which shows two spectra of

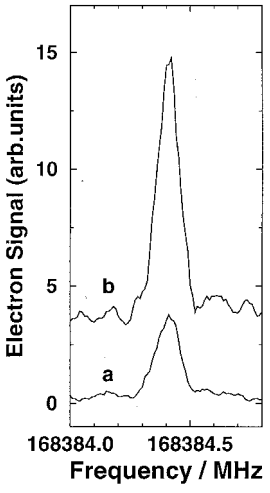

Figure 6. Measurement of the $92p[1/2](J=1) \quad 76d[3/2](J'=1)$ transition of argon using nozzle stagnation pressures of 1 bar (trace a) and 3 bar (trace b) leading to local pressures in the measurement region of *c*. 0.01 mbar and 0.03 mbar, respectively.

the $92p[1/2](J=1) \quad 76d[3/2](J'=1)$ transition in argon, measured using nozzle stagnation pressures of 1 bar (trace a) and 3 bar (trace b), leading to local pressures in the measurement region of *c*. 0.01 mbar and 0.03 mbar, respectively. Despite the threefold increase in the neutral argon density, no shift is detectable at the experimental resolution of 100 kHz.

3. Applications

3.1. *High-resolution millimetre wave spectroscopy of atomic Rydberg states*

We have tested our experimental procedure by recording millimetre wave spectra of Rydberg states of atomic argon [25] and krypton [37] below the lowest $^2P_{3/2}$ ionization limit. The Rydberg series that are optically accessible by single-photon absorption from the ground state are *s* and *d* series with $J=1$. Three series, the $ns[3/2](J=1)$, $nd[3/2](J=1)$ and $nd[1/2](J=1)$ series, converge to the $^2P_{3/2}$ limit, and two series, the $ns'[1/2](J=1)$ and $nd'[3/2](J=1)$ series, to the $^2P_{1/2}$ ionization limit [43]. Figures 7(*a*) and (*b*) show laser spectra of argon and krypton below the lowest ionization limit recorded at a resolution of 0.1–0.2 cm^{-1}. The spectra were recorded by monitoring the delayed PFI as a function of the XUV laser wavenumber. Examples of millimetre wave spectra are displayed in figures 7(*c*) and (*d*) which show spectra of the $62d[3/2](J'=1) \rightarrow 67f[k](J)$ transitions of argon and of the $77d[3/2](J'=1) \rightarrow 91f[k](J)$ transitions of krypton respectively [43]. The three lines observed in each millimetre wave spectrum correspond to the three optically accessible spin–orbit components of the *f* states. The lower doublet corresponds to transitions to $k=3/2$ and $J=1$ and 2 Rydberg states, and the upper line to a transition to the $k=5/2$ and $J=2$ Rydberg state. All isotopes of krypton contribute to the lines in figure 7(*d*), with the exception of the ^{83}Kr isotope whose transitions are shifted outside the spectral range displayed in figure 7(*d*) by the hyperfine interaction [48]. Measurements such as those presented in figure 7 demonstrate that one can obtain detailed information on the energy level structure,

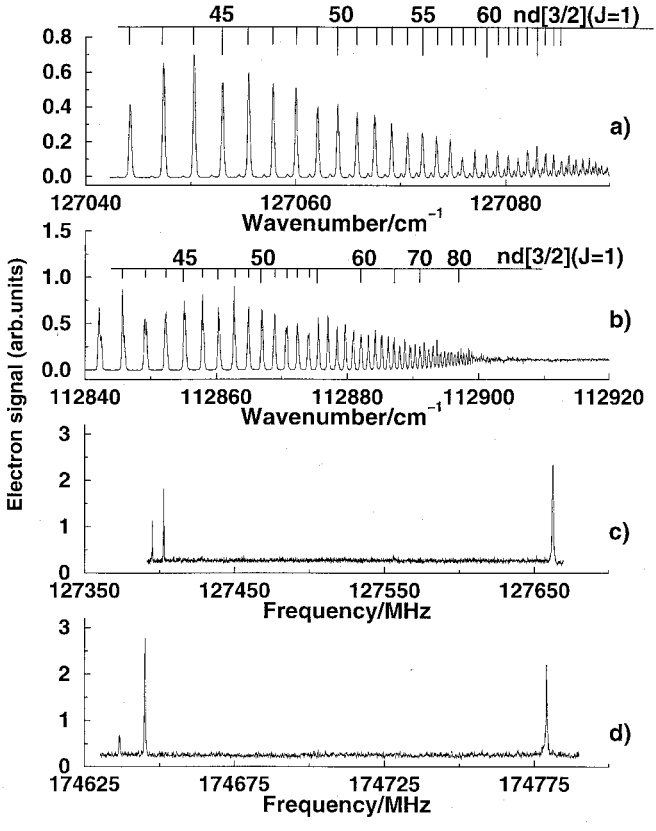

Figure 7. PFI spectra of (*a*) argon, and (*b*) krypton Rydberg states below the $^2P_{3/2}$ ionization limit using a tunable XUV laser source. The high-resolution millimetre wave spectrum of the $62d[3/2](J' = 1) \rightarrow 67f[k](J)$ transitions of argon and of the $77d[3/2](J' = 1) \rightarrow 91f[k](J)$ transitions of krypton are displayed in (*c*) and (*d*) respectively.

including spin–orbit and hyperfine interactions, up to high values of n, determine effective quantum defects accurately and extract information, from level shifts, on channel interactions. Stark maps at high values of n can also conveniently be measured [37].

3.2. *Millimetre wave spectroscopy of high Rydberg states and PFI–ZEKE photoelectron spectroscopy*

Figures 8(*a*) and (*b*) show millimetre wave spectra of high Rydberg states of argon and benzene with principal quantum numbers around 180 and 120 respectively. These states are located $3.3\,\mathrm{cm}^{-1}$ and $7.6\,\mathrm{cm}^{-1}$ below their series limit respectively, can be field ionized with pulsed electric fields of $0.8\,\mathrm{V\,cm}^{-1}$ and $3.6\,\mathrm{V\,cm}^{-1}$ and lie in the energy window typically probed by PFI–ZEKE photoelectron spectroscopy. The spectra in figure 8 were recorded under the normal conditions of operation of our PFI–ZEKE photoelectron spectrometer and provide useful information on the Rydberg states that we observe in PFI–ZEKE photoelectron spectroscopic experiments.

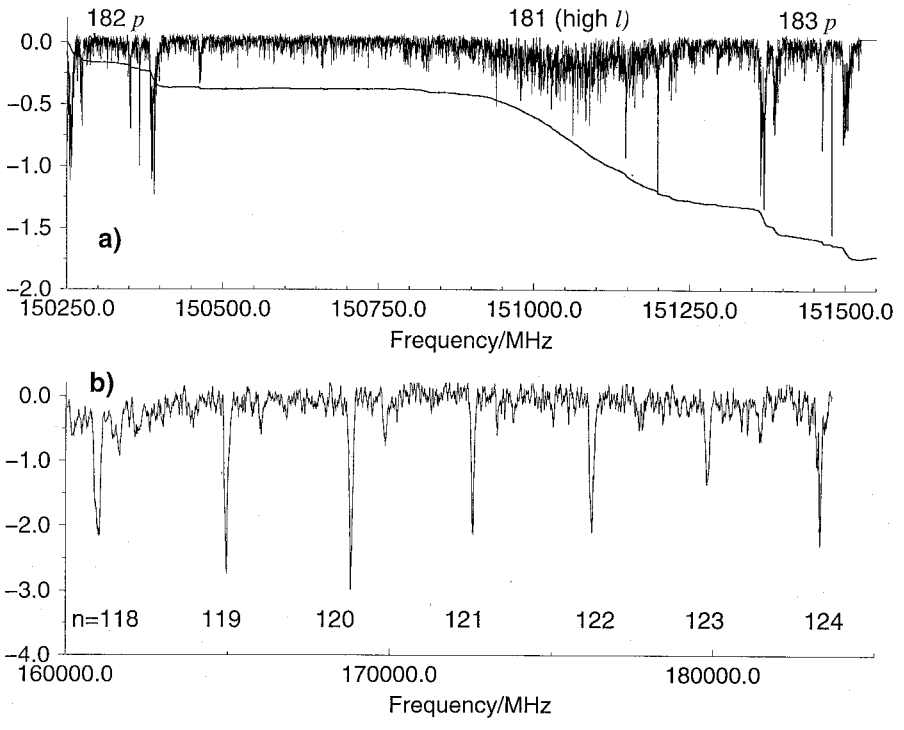

Figure 8. Millimetre wave spectra of (*a*) transitions between the $115d[3/2](J' = 1)$ Rydberg state and $n = 182$ and 183 Rydberg states of argon and (*b*) between an $n = 91$ Rydberg state of benzene and Rydberg states in the range $n = 118$–124.

The argon spectrum consists of two groups of six relatively sharp transitions between 150 250 and 150 500 MHz and between 151 350 and 151 550 MHz, which correspond to transitions from the $115d[3/2](J' = 1)$ Rydberg state to $n = 182p$ and $183p$ Rydberg states. Between these two groups of lines a broad feature centred around 151 070 MHz is also noticeable. This broad feature is caused by Stark mixing of the optically accessible f Rydberg states with the high-l manifold of Stark states. Because the quantum defects δ_f of the three optically accessible f Rydberg states in argon are smaller than 0.022 [25], the f states are mixed with, and immersed in, the high-l manifold of Stark states at electric fields greater than $350\,\mu V\,cm^{-1}$, i.e. at fields $F \geq 1.5\delta_f/n^5$. By comparing the full width ($\approx$200 MHz) of this broad unresolved feature with the expected width of $3n^2F$ (in atomic units) of the linearly expanding Stark manifold of high-l states one can estimate that the stray field in the apparatus amounts to approximately $1.5\,mV\,cm^{-1}$. One can also conclude from the inhomogeneously broadened asymmetric line shapes of the transitions to the p states that the electric field distribution is inhomogeneous across the excitation volume and is caused, to a large extent, by ions that are generated during the measurement cycles [37, 38].

Considering the integrated intensities (broad full line in figure 8(*a*)) leads to the conclusion that approximately 80% of the total PFI signal stems from the broad, unresolved feature that corresponds to the high-l manifold of Stark states and that only 20% is attributable to the p states. Because the Rydberg states of argon, located below the $^2P_{3/2}$ limit, cannot decay by autoionization or by predissociation, and

because the radiative decay is extremely slow at high n values, all states produced by the millimetre waves survive until the application of the pulsed field. In molecules, penetrating low-l Rydberg states (with $l = 0$–3) usually decay rapidly by predissociation, autoionization or internal conversion. One therefore expects that low-l states decay during the delay times of typically 1 μs used between photoexcitation and PFI in PFI–ZEKE photoelectron spectroscopy. The delay time thus acts as a filter that selects the long-lived non-penetrating Rydberg states that appear as the broad feature in figure 8(*a*).

This expectation is confirmed by the millimetre wave spectrum of benzene Rydberg states with $n = 118$–124 (figure 8(*b*)) which exclusively contains spectral features at the positions expected for transitions between states of zero quantum defects [38]: unlike the argon spectrum, this spectrum shows no trace of low-l states with non-vanishing quantum defects but consists of a single Rydberg series. Moreover, the lines have width in the range 100–200 MHz, which is almost a factor of 1000 broader than our experimental resolution. The initial $n = 91$ Rydberg state of the millimetre wave transitions was prepared in a two-photon excitation sequence from the ground S_0 state via the intermediate $|S_1\,6^1\rangle|2, 2, +l\rangle$ state. Only even l Rydberg states are optically accessible from the selected $|S_1\,6^1\rangle$ intermediate state. The s, and probably also the d, Rydberg states are expected to decay very rapidly by internal conversion [49]. The quantum defect of the g states is small enough that efficient mixing with the non-penetrating high-l manifold of Stark states takes place at stray fields of less than 2 mV cm^{-1} [38]. The lines observed in the millimetre wave spectrum therefore represent the broad envelope of transitions between Stark states at $n = 91$ and Stark states at $n = 118$–124.

From these results on argon and benzene the following conclusions can be drawn concerning the states that we observe in our PFI–ZEKE photoelectron spectrometer: Of the several optically accessible Rydberg series the most penetrating ones do not contribute to the PFI–ZEKE signals at n values in the range $n \leq 200$. The series with the highest l values are mixed with the high-l manifold of Stark states and become long lived if their quantum defect fulfils the condition $1.5n^2F \geq \delta_l/n^3$ (in atomic units). In our apparatus, the electric fields are mostly caused by ions produced during the experiment; they are small and inhomogeneous in nature. The equation

$$\left(\frac{9.14 \times 10^{15}|\delta_l|}{n^5}\right)^{3/2} \leq c/(\text{ions cm}^{-3}),$$

derived in [38], can be used to estimate the ion concentration necessary for the long-term stabilization of an initially prepared Rydberg state with principal quantum number n and quantum defect δ_l. For example, ion concentrations of 2×10^6 ions cm^{-3} are required to stabilize Rydberg states with $\delta_l = 0.004$ at $n \geq 70$ and Rydberg states with $\delta_l = 0.03$ at $n \geq 120$. An increase of the ion concentration thus results in the observation of lower Rydberg states and in a loss of resolution in PFI–ZEKE photoelectron spectra caused by the broadening of the lines on their low-frequency side [50].

3.3. *Millimetre wave spectroscopy and electric field measurements*

The spectroscopic investigation of high Rydberg states requires a good control over stray fields. A careful design of the experimental region (polished and widely spaced electrodes, magnetic shielding, etc.) is helpful in reducing stray fields. Equally

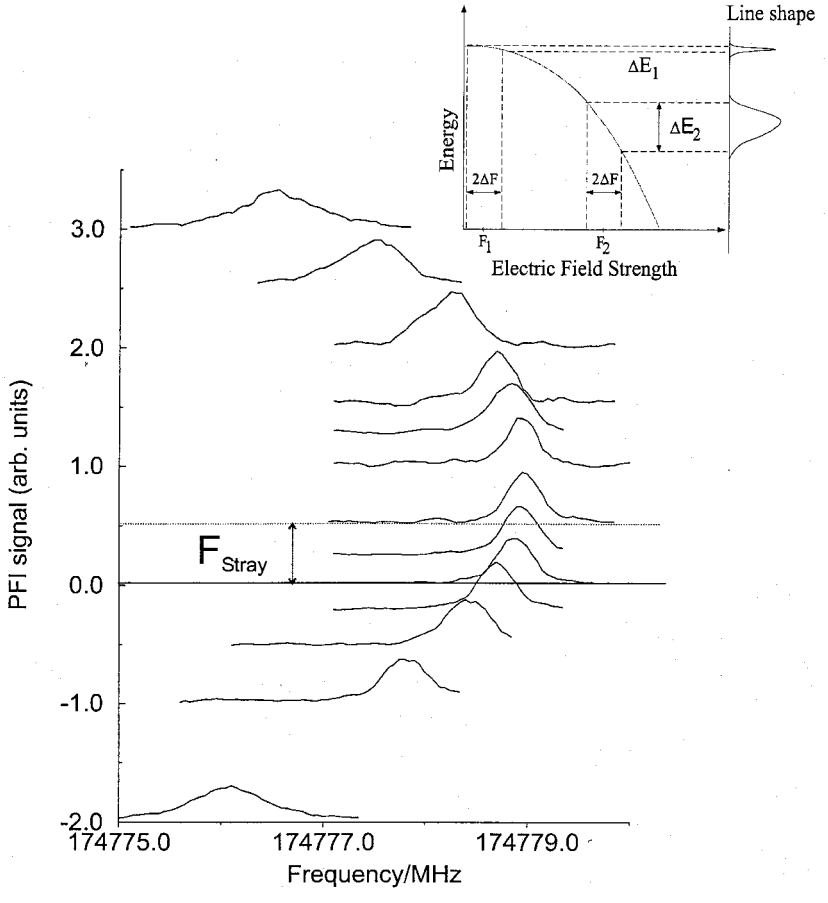

Figure 9. Measurements of electric fields and ion concentrations using millimetre wave spectroscopy of high Rydberg states. The spectra show the $n = 77d[3/2](J' = 1) \rightarrow 91f[5/2](J = 2)$ transition of krypton recorded at different applied electric fields. The horizontal axis of each spectrum has been shifted so that it intersects the vertical axis at the value of the applied electric field. Inset: schematic energy diagram illustrating the asymmetric broadening that results from inhomogeneous electric field distributions.

important, in pulsed experiments, is the synchronization of the measurement cycles with the 50 Hz frequency of the mains. The stray fields in our apparatus never exceed 1–3 mV cm^{-1} and can be compensated to less than 20 μV cm^{-1} by measuring and systematically minimizing the Stark shifts induced by intentionally applied fields, as is illustrated in figure 9.

The minimization procedure that we have developed specifically for our studies is described in detail in [37] and exploits the large polarizability of the high Rydberg states themselves. A millimetre wave transition between two high Rydberg states (here between the $n = 77d[3/2](J' = 1)$ and the $91f[5/2](J = 2)$ Rydberg states of the krypton atom) is recorded at high resolution as a function of the magnitude of an intentionally applied electric field. Because the spectral shift varies quadratically with the electric field strength, the line positions, when plotted as a function of the field strength, fall on a parabolic curve. At the apex of the parabola, the component of the

electric field in the direction of the applied field has been exactly compensated, and the value of the applied compensation field corresponds to the negative value of the stray field (here $-646 \pm 20\,\mu V\,cm^{-1}$).

This compensation procedure only removes the spatially homogeneous component of the field and is not suited to eliminate electric field inhomogeneities such as those caused by ions generated in the experimental volume. These inhomogeneities lead to an asymmetric inhomogeneous broadening of the spectral lines that becomes increasingly noticeable at increasing values of the electric field in figure 9. The reason for the asymmetric broadening lies in the quadratic dependence of the line positions on the local electric fields felt by the Rydberg atoms or molecules and is explained schematically in the inset of figure 9. The actual value of the electric field varies across the sample volume in a range represented schematically by two vertical dotted lines on both sides of the central field value (F_1 or F_2 in the figure). The broadening that results from the same inhomogeneous electric field distribution is more pronounced at larger electric fields.

In our experiments, electric field inhomogeneities originate primarily from charged particles in the experimental volume (see above). We can therefore analyse the line broadenings and line shapes to obtain the electric field distribution and, by means of the analytical expressions first introduced by Holtsmark [51, 52], obtain good estimates of the ion concentrations in the sample volume (see [37] for more details).

3.4. *Millimetre wave spectroscopy of high molecular Rydberg states*

Millimetre wave spectroscopy can also be used to study molecular Rydberg states. So far, we have been able to record millimetre wave spectra of high Rydberg states of H_2 [40, 41], N_2 [53] and C_6H_6 [38]. As an example, we summarize our recent investigation of the hyperfine structure of $l = 0$–3 Rydberg states of ortho H_2 in the range $n = 50$–65 [40, 41].

Many *nl* Rydberg states with $l = 0$–3 that belong to series converging on the first rotational levels of the $X\ ^2\Sigma_g^+(v^+ = 0)$ state of H_2^+ are long lived [54–56] and are ideally suited to high-resolution millimetre wave spectroscopy. To cleanly select Rydberg states of ortho (para) H_2, we prepare *ns* and *nd* Rydberg states in a two-photon excitation process via an even (odd) rotational level of the $B\ ^1\Sigma_u^+$ state. Figure 10(*a*) shows a laser spectrum of Rydberg states of ortho H_2 located below the ionization threshold that was obtained by selecting the $v = 3$, $J = 0$, rovibrational level of the B state. At the experimental resolution of $0.04\,cm^{-1}$ (1.3 GHz), the transitions to Rydberg states of ortho and para H_2 are equally broad and figure 10(*a*) therefore does not reveal any information about the hyperfine structure in ortho H_2. The hyperfine structure is easily resolved in millimetre wave spectra of ortho H_2 as is demonstrated in figures 10(*b*) and (*c*) which show survey spectra of transitions between the selected $n = 51d$ Rydberg state and 54 and 55 *p* and *f* Rydberg states located below the $v^+ = 0, N^+ = 1$ rotational level of the H_2^+ ion. When recorded at high resolution, each feature in figures 10(*b*) and (*c*) reveals a considerable substructure. As an example, figure 10(*d*) shows a high-resolution recording of the feature marked with an arrow in figure 10(*c*). The spectral richness of the millimetre wave spectra of ortho H_2, which is absent from the spectra of para H_2, has its origin in the hyperfine interaction.

The analysis of the spectra is facilitated by recording millimetre wave spectra from the same initial Rydberg states to two neighbouring sets of final Rydberg states

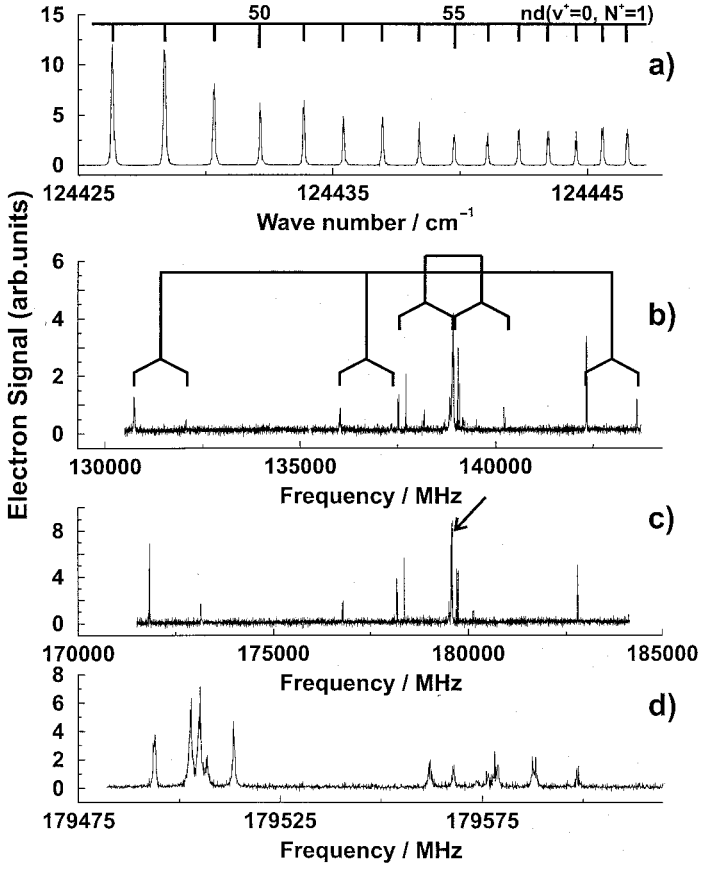

Figure 10. (*a*) PFI spectrum of *ns* and *nd* Rydberg states located below the $X\,^2\Sigma_g^+(v^+ = 0, N^+ = 1)$ state of ortho H_2^+ recorded in a two-photon excitation sequence via the $B\,^1\Sigma_u^+(v = 3, J = 0)$ state. (*b*) and (*c*) Millimetre wave spectra of transitions from the 51*d* Rydberg states and *p* and *f* Rydberg states at $n = 54$ and $n = 55$ respectively. (*d*) High-resolution scan of the line marked with an arrow in (*c*).

as shown in figures 10(*b*) and (*c*). In this way, combination differences can be extracted in the upper states [40]. Similarly, combination differences can be derived for the lower state by recording transitions from two neighbouring sets of initial levels of different *n* values to the same set of final states. Additional help in the assignment of the spectra is provided by the different behaviour of *p* and *f* Rydberg states in the presence of electric fields that can be used to determine the *l* value of the final state [40]. The coarse structure in the survey spectra is attributable to five groups of doublets separated by ≈1300 MHz. From combination differences this splitting can be assigned to an energy interval in the starting *nd* Rydberg states and corresponds approximately to the splitting between $G_c = 1/2$ and 3/2 levels of the H_2^+ ion [57] ($\boldsymbol{G}_c = \boldsymbol{S}_c + \boldsymbol{I}$, where $\boldsymbol{G}_c$ represents the angular momentum resulting from the addition of the electron spin $\boldsymbol{S}_c$ and the nuclear spin $\boldsymbol{I}$ of the H_2^+ core). Of the five groups of doublets, the lowest two and the highest one are attributed to transitions to *p* Rydberg states and the remaining two to transitions, which are also separated by approximately 1300 MHz, to *nf* Rydberg states. The analysis of the

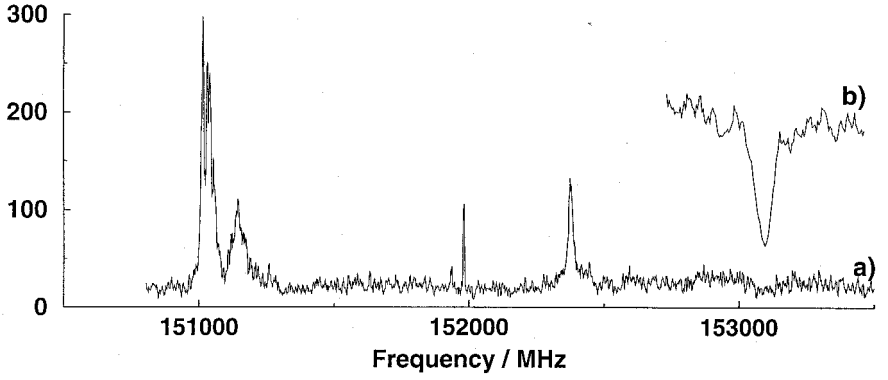

Figure 11. Section of the millimetre wave spectrum from the $n = 48d$ Rydberg states of H_2 to $n = 51$ Rydberg states. (*a*) The SFI signal of the final states of the millimetre wave transitions and (*b*) the SFI signal of the initial state.

hyperfine structure in these millimetre wave spectra can be extrapolated to the hyperfine structure in the ground state of ortho H_2^+ with a precision of better than 1 MHz [41].

By following the evolution of the spectral and energy level structures as a function of n and l one can also observe how the angular momentum coupling hierarchy gradually evolves and the Rydberg electron becomes decoupled from the motion of the ion core. For instance, at the n values investigated in figure 10 ($n \approx 50$), the hyperfine interaction has already caused the *nd* and *nf* Rydberg states to be of mixed singlet ($S = 0$) and triplet ($S = 1$) character whereas the more penetrating *ns* and *np* Rydberg states can still be described by a well-defined total electron spin [40]. At low values of n ($n = 3$ or 4) the *s*, *p* and *d* singlet and triplet states are still observable as distinct electronic states [58–60]. The mixing of singlet and triplet character in *f* Rydberg states starts being observed at $n = 4$ already [61].

The short lifetimes of molecular Rydberg states can pose problems for high-resolution millimetre wave spectroscopy. If the initial state is short lived, it is necessary to increase the millimetre wave intensities to observe the transitions. Moreover, the linewidths are broad, which prevents an optimal use of the high resolution of the method. If the final state is short lived one does not observe any signal by SFI of the final state of the millimetre wave transition. In this case, it is advantageous to record the SFI signal of both initial state and final state of the millimetre wave transitions simultaneously by setting gates in the electron TOF spectra. Transitions to short-lived upper states are then detected as dips in the SFI signal of the initial state as is illustrated in figure 11. The width of the dips can be converted into a lifetime or a predissociation (autoionization) decay rate for the upper level. In H_2 we have occasionally observed that neighbouring hyperfine components have lifetimes that differ by more than two orders of magnitude which suggests either very local perturbations or restrictive selection rules for the decay process involved.

Measurements such as those presented in figures 10 and 11 illustrate the power of millimetre wave spectroscopy to investigate the properties of highly excited molecular electronic states. The wealth of spectral structures and behaviours observed so far indicates that the current understanding of molecular Rydberg states is still far from complete, even in the case of molecules as small as H_2.

Although the results presented for H_2 represent an important step in the study of high molecular Rydberg states, some difficulties remain to be overcome before the measurements can be extended to other molecules in a straightforward way. The main restriction so far comes from the short lifetimes of low-l Rydberg states in most molecular systems. Multiphoton excitation schemes may enable less penetrating states with longer lifetimes to be reached. Recently, Gallagher and coworkers have used microwave radiation to stabilize high Rydberg states of the NO molecule [62]. Alternatively, Rydberg states of higher l values can be prepared by using single-photon excitation in the presence of an electric field that is brought back to zero after photoexcitation.

4. Conclusions

Millimetre wave spectroscopy is a powerful method to study Rydberg states of atoms and molecules at very high resolution. The measurement of line shifts and line broadenings in millimetre wave spectra of high Rydberg states provides a very sensitive diagnostic of electric fields and ion concentrations in an experimental apparatus. Millimetre wave spectroscopy of molecular Rydberg states can be used to obtain new information on the energy level structure at high n values, including the hyperfine structure. The measured hyperfine structure at a given value of n, in combination with a suitable angular momentum frame transformation, provides a reliable method of determining the hyperfine structure in molecular ions [41]. Millimetre wave spectroscopy of $n = 100$–200 Rydberg states is also helpful in assessing the experimental conditions under which PFI–ZEKE photoelectron spectroscopy experiments are performed and in understanding the nature of the Rydberg states that are field ionized in these experiments. This understanding has been helpful in recent experiments in which the resolution of PFI-ZEKE photoelectron spectroscopy has been improved to better than $0.05\,cm^{-1}$ [39, 63].

Acknowledgments

Our research is funded by the ETH Zurich and the Swiss National Science Foundation under project no. 21-61682.00.

References

[1] Stebbings, R. F., and Dunning, F. B. (editors), 1983, *Rydberg States of Atoms and Molecules* (Cambridge: Cambridge University Press).
[2] Gallagher, T. F., 1994, *Rydberg Atoms* (Cambridge: Cambridge University Press).
[3] Connerade, J. P., 1998, *Highly Excited Atoms* (Cambridge: Cambridge University Press).
[4] Schramm, A., Weber, J. M., Kreil, J., Klar, D., Ruf, M.-W., and Hotop, H., 1998, *Phys. Rev. Lett.*, **81**, 778.
[5] Brevet, P. F., Pellarin, M., and Vialle, J. L., 1990, *Phys. Rev.* A, **42**, 1460.
[6] Goy, P., Fabre, C., Gross, M., and Haroche, S., 1980, *J. Phys.* B, **13**, L83.
[7] Gallagher, T. F., Hill, R. M., and Edelstein, S. A., 1976, *Phys. Rev.* A, **14**, 744.
[8] Wing, W., and MacAdam, K., 1978, in *Progress in Atomic Spectroscopy* (Vol. A), edited by H. Hanle and W. Kleinpoppen (New York: Plenum Press), chap. 11.
[9] Rubbmark, J. R., Kash, M. M., Littman, M. G., and Kleppner, D., 1981, *Phys. Rev.* A, **23**, 3107.
[10] Fabre, C., Haroche, S., and Goy, P., 1978, *Phys. Rev.* A, **18**, 229.
[11] Frey, M. T., Ling, X., Lindsay, B. G., Smith, K. A., and Dunning, F. B., 1993, *Rev. sci. Instrum.*, **64**, 3649.

[12] Frey, M. T., Hill, S. B., Smith, K. A., Dunning, F. B., and Fabrikant, I. I., 1995, *Phys. Rev. Lett.*, **75**, 810.
[13] Hotop, H., Klar, D., Ruf, M.-W., Schramm, A., and Weber, J. M., 1995, in *The Physics of Electronic and Atomic Collisions*, AIP Conference Proceedings, Vol. **360**, p. 267.
[14] Weber, J. M., Ueda, K., Klar, D., Kreil, J., Ruf, M.-W., and Hotop, H., 1999, *J. Phys.* B, **32**, 2381.
[15] Bömmels, J., Weber, J. M., Gopalan, A., Herschbach, N., Leber, E., Schramm, A., Ueda, K., and Hotop, H., 1999, *J. Phys.* B, **32**, 2399.
[16] Beigang, R., Makat, W., Timmermann, A., and West, P. J., 1983, *Phys. Rev. Lett.*, **51**, 771.
[17] Beigang, R., 1985, *Comments at. mol. Phys.*, **16**, 117.
[18] Neukammer, J., Rinneberg, H., Vietzke, K., König, A., Hieronymus, H., Kohl, M., Grabka, H.-J., and Wunner, G., 1987, *Phys. Rev. Lett.*, **59**, 2947.
[19] Sturrus, W. G., Sobol, P. A., and Lundeen, S. R., 1985, *Phys. Rev. Lett.*, **54**, 792.
[20] Sturrus, W. G., Hessels, E. A., Arcuni, P. W., and Lundeen, S. R., 1988, *Phys. Rev. Lett.*, **61**, 2320.
[21] Arcuni, P. W., Fu, Z. W., and Lundeen, S. R., 1990, *Phys. Rev.* A, **42**, 6950.
[22] Jacobson, P. L., Fischer, D. S., Fehrenbach, C. W., Sturrus, W. G., and Lundeen, S. R., 1998, *Phys. Rev.* A, **56**, R4361.
[23] Palm, H., and Merkt, F., 1998, *Appl. Phys. Lett.*, **73**, 157.
[24] Hollenstein, U., Palm, H., and Merkt, F., 2000, *Rev. sci. Instrum.*, **71** 4023.
[25] Merkt, F., and Schmutz, H., 1998, *J. chem. Phys.*, **108**, 10033.
[26] Reiser, G., Habenicht, W., Müller-Dethlefs, K., and Schlag, E. W., 1988, *Chem. Phys. Lett.*, **152**, 119.
[27] Bahatt, D., Even, U., and Levine, R. D., 1993, *J. chem. Phys.*, **98**, 1744.
[28] Chupka, W. A., 1993, *J. chem. Phys.*, **98**, 4520.
[29] Merkt, F., and Softley, T. P., 1993, *Int. Rev. phys. Chem.*, **12**, 205.
[30] Schlag, E. W., 1998, *ZEKE Spectroscopy* (Cambridge: Cambridge University Press).
[31] Remacle, F., and Levine, R. D., 1996, *J. chem. Phys.*, **105**, 4649.
[32] Merkt, F., and Zare, R. N., 1994, *J. chem. Phys.*, **101**, 3495.
[33] Bixon, M., and Jortner, J., 1995, *J. chem. Phys.*, **103**, 4431.
[34] Vrakking, M. J. J., 1996, *J. chem. Phys.*, **105**, 7336.
[35] Procter, S. R., Webb, M. J., and Softley, T. P., 2000, *Faraday Discuss. Chem. Soc.*, **115**, 277.
[36] Softley, T. P., and Rednall, R. J., 2000, *J. chem. Phys.*, **112**, 7992.
[37] Osterwalder, A., and Merkt, F., 1999, *Phys. Rev. Lett.*, **82**, 1831.
[38] Osterwalder, A., Willitsch, S., and Merkt, F., 2001, *J. mol. Struct.*, **599**, 163.
[39] Hollenstein, U., Seiler, R., Schmutz, H., Andrist, M., and Merkt, F., 2001, *J. chem. Phys.*, **115**, 5461.
[40] Osterwalder, A., Seiler, R., and Merkt, F., 2000, *J. chem. Phys.*, **113**, 7939.
[41] Osterwalder, A., Wüest, A., Merkt, F., and Jungen, Ch., in preparation.
[42] Merkt, F., Osterwalder, A., Seiler, R., Signorell, R., Palm, H., Schmutz, H., and Gunzinger, R., 1998, *J. Phys.* B, **31**, 1705.
[43] Moore, C. E., 1949, *Atomic energy Levels*, Vol. 1 (NBS circular 467) (Washington, DC: US Government Printing Office).
[44] Kneubühl, F., 1994, *Repetitorium der Physik* (Stuttgart: Teubner).
[45] Amaldi, E., and Segrè, E., 1934, *Nuovo Cimento*, **11**, 145.
[46] Fermi, E., 1934, *Nuovo Cimento*, **11**, 157.
[47] Herzberg, G., and Jungen, Ch., 1972, *J. mol. Spectrosc.*, **41**, 425.
[48] Merkt, F., Signorell, R., Palm, H., Osterwalder, A., and Sommavilla, M., 1998, *Mol. Phys.*, **95**, 1045.
[49] Chupka, W. A., 1993, *J. chem. Phys.*, **99**, 5800.
[50] Palm, H., and Merkt, F., 1997, *Chem. Phys. Lett.*, **270**, 1.
[51] Holtsmark, J., 1919, *Ann. Phys.*, **58**, 577.
[52] Holtsmark, J., 1924, *Phys. Z.*, **25**, 73.
[53] Greetham, G. M., and Merkt, F., in preparation.

[54] FREUND, R. S., 1983, in *Rydberg States of Atoms and Molecules*, edited by R. F. Stebbings and F. B. Dunning (Cambridge: Cambridge University Press), p. 355.
[55] ROTTKE, H., and WELGE, K., 1992, *J. chem. Phys.*, **97**, 908.
[56] MERKT, F., XU, H., and ZARE, R. N., 1996, *J. chem. Phys.*, **104**, 950.
[57] JEFFERTS, K. B., 1969, *Phys. Rev. Lett.*, **23**, 1476.
[58] LICHTEN, W., WIK, T., and MILLER, T. A., 1979, *J. chem. Phys.*, **71**, 2441.
[59] JÓZEFOWSKI, L., OTTINGER, CH., and ROX, T., 1994, *J. mol. Spectrosc.*, **163**, 381.
[60] OTTINGER, CH., ROX, T., and SHARMA, A., 1994, *J. mol. Spectrosc.*, **163**, 414.
[61] UY, D., GABRYS, C. M., OKA, T., COTTERELL, T., STICKLAND, R. J., JUNGEN, CH., and WÜEST, A., 2000, *J. chem. Phys.*, **113**, 10143.
[62] MURGU, E., MARTIN, J. D. D., and GALLAGHER, T. F., 2001, *J. chem. Phys.*, **115**, 7032.
[63] HOLLENSTEIN, U., SEILER, R., OSTERWALDER, A., SOMMAVILLA, M., WÜEST, A., RUPPER, P., WILLITSCH, S., GREETHAM, G. M., BRUPBACHER-GATEHOUSE, B., and MERKT, F., 2001, *Chimia*, **55**, 759.